Pressure effect on magnetic hysteresis parameters of single-domain magnetite contained in natural plagioclase crystal

Geophysical Journal International

Geophys. J. Int. (2015) **202,** 394–401 doi: 10.1093/gji/ggv154

GJI Geomagnetism, rock magnetism and palaeomagnetism

Pressure effect on magnetic hysteresis parameters of single-domain magnetite contained in natural plagioclase crystal

Masahiko Sato,[1,2] Yuhji Yamamoto,[3] Takashi Nishioka,[4] Kazuto Kodama,[3] Nobutatsu Mochizuki,[5] Yoichi Usui[6] and Hideo Tsunakawa[2]

[1]*Department of Environmental Changes, Faculty of Social and Cultural Studies, Kyushu University,* 744 *Motooka, Nishi-ku, Fukuoka* 819-0395, *Japan. E-mail: m.sato@scs.kyushu-u.ac.jp*

[2]*Department of Earth and Planetary Sciences, Tokyo Institute of Technology,* 2-12-1 *Ookayama, Meguro-ku, Tokyo* 152-8550, *Japan*

[3]*Center for Advanced Marine Core Research, Kochi University, B*200 *Monobe, Kochi* 783-8502, *Japan*

[4]*Graduate School of Integrated Arts and Sciences, Kochi University,* 2-5-1 *Akebono-cho, Kochi* 780-8520, *Japan*

[5]*Priority Organization for Innovation and Excellence, Kumamoto University,* 2-39-1 *Kurokami, Chuo-ku, Kumamoto* 860-8555, *Japan*

[6]*Japan Agency for Marine-Earth Science and Technology,* 2-15 *Natsushima-cho, Yokosuka* 237-0061, *Japan*

Accepted 2015 April 8. Received 2015 March 24; in original form 2014 October 5

SUMMARY

This study investigates pressure effects on the magnetic properties of non-interacting single-domain (SD) magnetite. Using a high-pressure cell specially designed for a Magnetic Property Measurement System, magnetic hysteresis measurements were conducted under high pressures of up to 1 GPa on natural plagioclase crystals containing much acicular SD magnetite. Coercivity and saturation magnetization were nearly constant with pressure, while saturation remanent magnetization and coercivity of remanence decreased with pressure at moderate rates of −8 per cent GPa^{-1} and −18 per cent GPa^{-1}, respectively. These results suggest that temperature effects govern the magnetic behaviour of acicular SD magnetite grains in the middle and lower crusts.

Key words: Magnetic anomalies: modelling and interpretation; Rock and mineral magnetism; High-pressure behaviour.

1 INTRODUCTION

Silicate minerals such as plagioclase and pyroxene sometimes contain fine-grained magnetite crystals; such silicates are called magnetic silicates. Magnetic silicates are ubiquitous in mafic and intermediate plutonic rocks (Dunlop & Özdemir 1997; Gee & Kent 2007). For a 40-km-thick average continental crust (Christensen & Mooney 1995; Rudnick & Fountain 1995), the middle crust ranges in depth from 12 to 23 km and the lower crust ranges in depth from 23 to 40 km (Rudnick & Gao 2003), although the depth and thickness of both middle and lower crusts vary from setting to setting. As the middle and lower crusts have greater mafic composition than the upper crust (Rudnick & Gao 2003), magnetic silicates should play an important role in controlling the magnetic properties of middle and lower crustal rocks. For understanding the sources of the long-wavelength magnetic anomalies over continental areas, which are considered to originate from thick magnetized layers within the crust (Shive *et al.* 1992 and reference therein), it is crucial to investigate the magnetic properties of fine-grained magnetite under conditions similar to the high temperature and pressure of the middle and lower crusts.

Magnetic hysteresis parameters, which provide fundamental information concerning magnetic properties, have been investigated at various temperatures for magnetite (e.g. Hodych 1982; Heider *et al.* 1987). However, because of the associated technical difficulties, few studies have been performed *in situ* hysteresis measurements of magnetite under hydrostatic pressure (Carmichael 1969; Gilder *et al.* 2002; Sato *et al.* 2014). Gilder *et al.* (2002) undertook *in situ* measurements of alternating current (AC) susceptibility under high pressure in a diamond anvil cell for single-domain (SD) and multidomain (MD) magnetite. In their experiment, coercivity (B_c) and saturation remanent magnetization (M_{rs}) of the SD magnetite increased slightly with pressure up to 1.3 GPa, and significant changes occurred above this pressure threshold. For the MD magnetite, they found no significant change in B_c and M_{rs} up to a pressure of 5.6 GPa at the resolution of their experiments. They used the integral of AC susceptibility to calculate hysteresis loops. As the integration of AC susceptibility is not a direct measurement of hysteresis parameters, it is desirable to conduct direct hysteresis measurements under high pressure for evaluating hysteresis parameters more reliably.

Sato *et al.* (2014) conducted *in situ* magnetic hysteresis measurement under high pressures of up to 1 GPa on MD magnetite using a high-pressure cell specially designed for a Magnetic Property Measurement System (MPMS). The pressure dependences they reported are as follows: B_c increases monotonously with pressure at a rate of +91 per cent GPa^{-1}, and M_{rs} increases with pressure

up to 0.5 GPa by ∼30 per cent until it appears to reach saturation. These pressure dependences are significantly different from those reported by Gilder *et al.* (2002). Therefore, direct measurements of the hysteresis parameters for SD magnetite are clearly required.

About the studied sample, Gilder *et al.* (2002) used chiton teeth as the SD magnetite sample. It is reported that the magnetite crystals in chiton teeth are closely packed against one another, separated only by a film (<0.05 μm) of organic material (Kirschvink & Lowenstam 1979). Such a short distance between the magnetite crystals might result in local fields of the order of several tens of milliteslas, and thus, their magnetic behaviour might differ greatly from isolated grains such as magnetic minerals contained in natural rocks (Kirschvink & Lowenstam 1979; Cisowski 1981).

In this study, to investigate the magnetic properties of SD magnetite contained within middle and lower crustal rocks, *in situ* magnetic hysteresis measurements under high pressures of up to 1 GPa were conducted using the high-pressure cell designed for an MPMS (Sato *et al.* 2012). The plagioclase crystals containing non-interacting SD magnetite were prepared from an ophiolitic gabbro and used as experimental samples. Based on the experimental results, we report the pressure dependences of magnetic hysteresis parameters for SD magnetite.

2 SAMPLE

We sampled a layered gabbro from the southern part of the Oman ophiolite (Sumail massif; 23.47°N, 58.19°E). Layered gabbros are considered to originate from the lower part of the oceanic crust (Kelemen *et al.* 1997 and references therein). Natural plagioclase samples were prepared from the layered gabbro using the following procedure. (1) The gabbro sample was crushed into mineral grains. (2) The mineral grains were soaked in hydrochloric acid for half a day. (3) The mineral grains were washed in an ultrasonic bath with pure water. (4) Plagioclase grains were picked by hand under a stereoscopic microscope.

Polished surfaces of the plagioclase grains were observed using a JSM-6500F Field Emission Scanning Electron Microscope (FE-SEM, JEOL) equipped with an energy-dispersive X-ray spectroscopy (EDS) option. There were abundant magnetite inclusions. Sizes of the inclusions were less than a few micrometers. The magnetite inclusions showed a wide variety of aspect ratios from 1 to 10 with an average of 2.5, about 10 per cent of which had low aspect ratios (<1.2). They were composed mainly of Fe, Ti and O, although point analyses by EDS could not completely resolve the inclusions from their surroundings because of their tiny inclusion sizes. The ulvöspinel content x ($Fe_{3-x}Ti_xO_4$) estimated from the Ti/Fe ratio was about 0.1. Additionally, there were high Ti/Fe ratio inclusions in the plagioclase crystals, which were considered to be ilmenite. The averaged value of the Ca/Na ratio for the plagioclase grains was about 10.

SD magnetite characteristics of magnetic minerals contained in the plagioclase sample were confirmed by rock-magnetic observations. A strong-field thermomagnetic curve of the plagioclase samples was measured between 100 and 700 °C under vacuum conditions (∼3 Pa) using an NMB-89 Magnetic Balance (Natsuhara-Giken). The cooling curve was slightly different from the heating curve due to the thermal alteration during heating (Fig. 1a). The observed Curie temperature (T_C) during heating was 548 °C, indicating low-Ti titanomagnetite. The ulvöspinel content estimated from the T_C was $x = 0.047$ (Hunt *et al.* 1995). This value is consistent with the value estimated from the EDS result. Magnetic hysteresis curves were measured using a MicroMag 3900 Vibrating Sample Magnetometer (VSM, Princeton Measurements Corporation). The obtained hysteresis parameters show SD characteristics on the Day

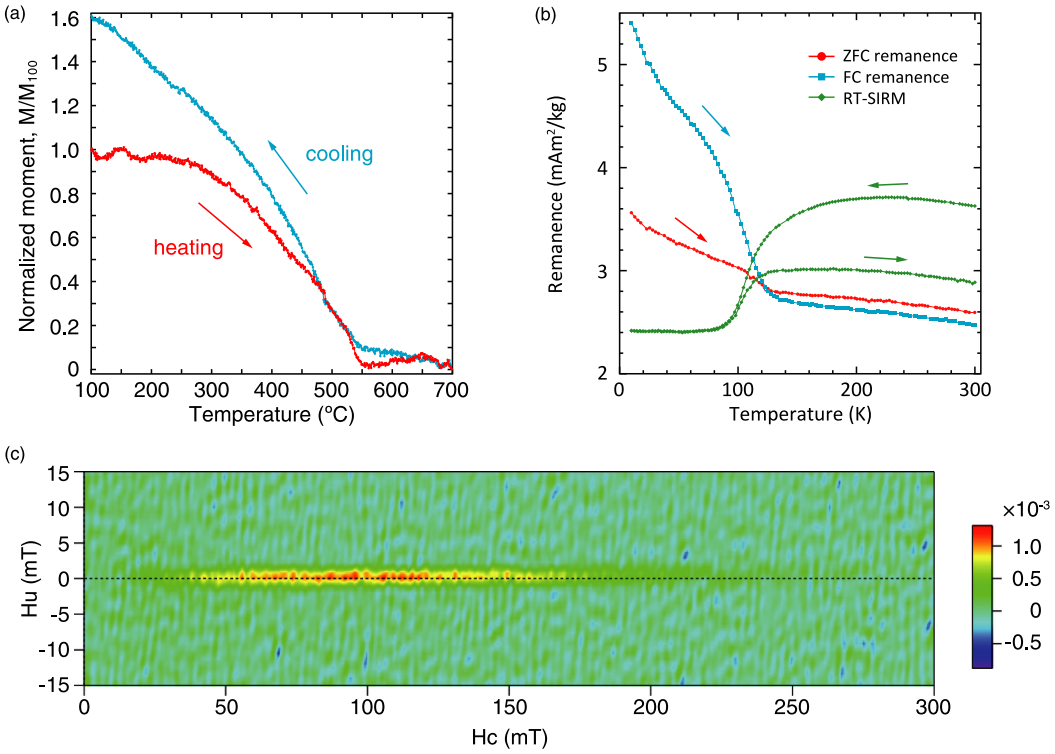

Figure 1. Rock-magnetic measurements of the plagioclase sample: (a) strong-field thermomagnetic curve, (b) low-temperature measurements and (c) FORC diagram. The FORC diagram is calculated using a smoothing factor of 3.

Table 1. Summary of the VSM measurement.

Sample state	B_c (mT)	M_{rs} (nAm^2)	M_s (nAm^2)	B_{cr} (mT)	M_{rs}/M_s	B_{cr}/B_c
Original	53.9	70.2	157	102	0.446	1.89
After pressurization	57.6	77.7	160	99.2	0.487	1.72

et al. (1977) plot (Table 1). The M_s value of 7.04×10^{-3} Am^2 kg^{-1} at room temperature indicates magnetite content in the plagioclase samples of 81 ppm (assuming the ulvöspinel content $x = 0.047$).

SD magnetite characteristics of magnetic minerals in the plagioclase sample were also observed in low-temperature experiments using an MPMS (Fig. 1b). The following low-temperature measurements were conducted: (1) thermal demagnetization during zero-field warming (ZFW) for an isothermal remanent magnetization (IRM) imparted in a field of 2.5 T at 10 K after zero-field cooling from 300 K (ZFC remanence); (2) thermal demagnetization during ZFW for a remanence given by field cooling from 300 to 10 K in a field of 2.5 T (FC remanence); and (3) low-temperature demagnetization (LTD) cycle for saturation IRM (SIRM) imparted in a field of 2.5 T at 300 K (RT-SIRM). These curves show pronounced remanence reductions at around 100–120 K, suggesting the Verwey transition of low-Ti titanomagnetite (Moskowitz *et al.* 1998). The intensity of FC remanence was larger than that of ZFC remanence, which is characteristic behaviour of SD and fine-grain pseudo-SD (PSD) magnetite (Moskowitz *et al.* 1993; Kosterov 2003; Carter-Stiglitz *et al.* 2006). As the RT-SIRM at 300 K reduced about 20 per cent after the LTD cycle, the plagioclase sample contained small amounts of nearly equidimensional SD magnetite (fig. 5 in Özdemir *et al.* 2002), whose magnetic properties are governed by magnetocrystalline anisotropy. This is consistent with the aspect ratio data of the FE-SEM observation.

A first-order reversal curve (FORC) for the plagioclase sample was measured using a MicroMag 2900 Alternating Gradient Magnetometer (AGM, Princeton Measurements Corporation), and the FORC diagram (Roberts *et al.* 2000) was calculated using FORCinel software (Harrison & Feinberg 2008). The FORC diagram showed a narrow horizontal ridge along $H_u = 0$ (Fig. 1c), suggesting that the plagioclase crystal contained non-interacting SD particles (Roberts *et al.* 2000).

3 HIGH-PRESSURE EXPERIMENT

The piston-cylinder type of high-pressure cell used in the present study was made of beryllium–copper alloy (BeCu) and zirconium oxide (ZrO_2), which is the same as that used by Sato *et al.* (2014). The plagioclase grains of 10.4 mg (~40 grains), glass wool, cylinder of resin and small chip of indium were placed in a Teflon capsule filled with a liquid pressure-transmitting medium (1:1 mixture of Fluorinert No. FC70 and No. FC77). Note that the plagioclase grains were placed with the glass wool. While slight rotation of the grains during the experiment was possible, it seems to be sufficiently small not to affect the experimental results. A 0.5-mm-thick Teflon disk was inserted below the Teflon capsule to prevent leakage of the pressure-transmitting liquid.

Superconducting transition temperatures of indium (~3 K) were measured before the sample measurements, and the nominal pressure values were calculated from changes in the transition temperatures (Jennings & Swenson 1958). Because the bulk modulus of the plagioclase crystals (~80 GPa for $Ab_{10}An_{90}$; Angel 2004) is smaller than that of magnetite (~200 GPa; Haavik *et al.* 2000 and references therein), it is reasonable to consider that pressure applied to the magnetite inclusions would be the same as that applied to the plagioclase matrix.

To check the pressure difference between about 3 and 300 K, we measured the Curie temperature of gadolinium (~295 K at 0 GPa), which is also known as a function of pressure (McWhan & Stevens 1965). Instead of the plagioclase sample, a chip of gadolinium was placed in the Teflon capsule, and the superconducting transition temperature of indium at around 3 K and the Curie temperature of gadolinium at around 300 K were measured at various pressures. The results indicate that the pressure differences were sufficiently small, especially smaller than 0.06 GPa in the range of >0.5 GPa (Fig. 2).

In the high-pressure experiment of the plagioclase sample, the applied pressure was changed at room temperature after the completion of each measurement cycle. One measurement cycle consisted of the following steps:

(1) cooling in zero-field from 300 to 3 K;
(2) measuring the transition temperature of indium around 3 K;
(3) warming in zero-field from 3 to 300 K;
(4) measuring a magnetic hysteresis loop at 300 K;
(5) imparting SIRM in a field of 500 mT;
(6) measuring a direct field demagnetization curve for SIRM with 20 mT steps.

The maximum field in the hysteresis loop measurement was 500 mT, sufficiently larger than the coercivity of SD magnetite with uniaxial anisotropy (<300 mT). A field increment was taken to be 5 mT when the applied field was close to zero, and it was set to be 10 or 20 mT in other cases. All magnetic measurements with the high-pressure cell were performed using an MPMS-XL5

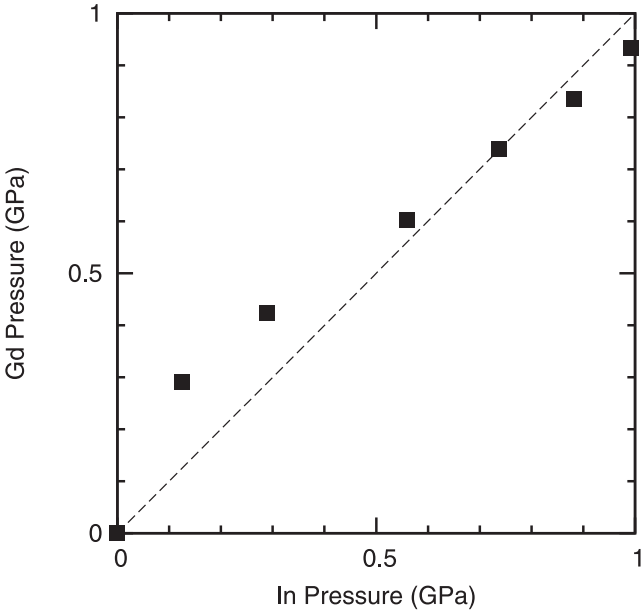

Figure 2. The relationship between the pressure at about 3 K (In Pressure) and the pressure at about 300 K (Gd Pressure). The dashed line indicates unity slope.

instrument at the Center for Advanced Marine Core Research, Kochi University.

In a magnetization measurement of the MPMS, the magnetic field generated by a sample is sensed along one direction. Then, the obtained signal is fitted to an ideal dipole signal for the MPMS sensor to calculate the magnetization of the sample. In our experiment, prior to the plagioclase sample measurements, a high-pressure cell without a plagioclase sample was subjected to the measurement cycle to obtain data for background subtractions. A Teflon capsule filled with the Fluorinert (without indium, resin, glass wool and sample) was placed into the high-pressure cell, and background data were collected in the same manner as for the plagioclase sample measurements without pressurization. In the plagioclase measurements, the signal of the high-pressure cell was subtracted from the measured signal (high-pressure cell + plagioclase sample) to calculate the magnetization of the plagioclase sample.

To assess reliability of the hysteresis measurements using the high-pressure cell, magnetic hysteresis loops of the plagioclase sample with a gelatin capsule were measured with the VSM both before and after the high-pressure experiment.

4 RESULTS

Fig. 3(a) shows an example of the background subtraction. Background-subtracted data for a single 6-cm scan show a nearly ideal dipolar signal (symmetric shape with minimum-to-minimum width of 3 cm), while raw data of the plagioclase sample in the high-pressure cell show an irregular shape because of the comparable magnetization between the sample and the cell. In the present study, the background subtraction always gave dipolar signals, irrespective of pressure and applied field values. This is consistent with the fact that changes in the cell length (ΔL) were substantially smaller than the entire cell length (L) during the high-pressure experiment ($\Delta L/L \sim 3$ per cent; Table 2), and thus, the signal of the cell does not appear to change under pressurization.

Hysteresis loops measured at ambient pressure are shown in Fig. 3(b). The hysteresis loop obtained using the MPMS and high-pressure cell is identical to that obtained using the VSM. Furthermore, the hysteresis parameters obtained using the MPMS and high-pressure cell show good agreement with the VSM measurement (Tables 1 and 2). For characterizations of the hysteresis parameters, a diamagnetic/paramagnetic correction was performed by

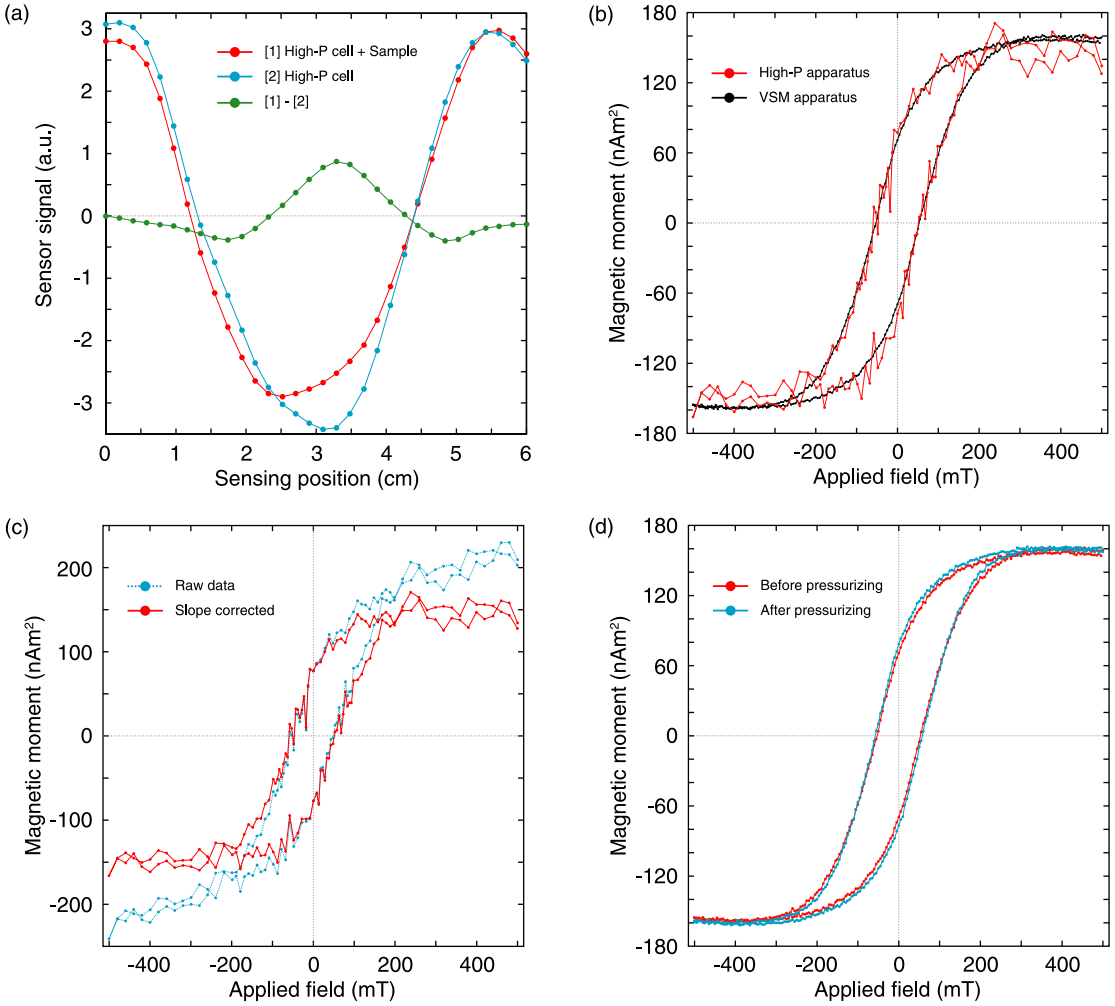

Figure 3. (a) Example of the background subtraction (pressure, $P = 0$ GPa; applied field, $B = +500$ mT). The MPMS sensor signal is plotted as a function of sensing position in the magnetization measurement. (b) Magnetic hysteresis loops for the plagioclase sample measured using the MPMS and high-pressure cell, and that measured using the VSM. The hysteresis loops were corrected by subtracting diamagnetic/paramagnetic slopes. (c) An example of the diamagnetic/paramagnetic slope correction ($P = 0$ GPa). (d) Magnetic hysteresis loops for the plagioclase sample measured before and after the high-pressure experiment.

Table 2. Summary of the MPMS high-pressure experiment.

P (GPa)	B_c (mT)	M_{rs+} [a] (nAm^2)	M_{rs-} [a] (nAm^2)	M_{rs_Bcr} [b] (nAm^2)	M_{rs_ave} [c] (nAm^2)	ΔM_{rs} [d] (nAm^2)	M_s (nAm^2)	σ_{Ms} (nAm^2)	B_{cr} (mT)	M_{rs}/M_s	B_{cr}/B_c	Slope (nAm^2/T)	L (mm)
0	52.1	77.2	77.5	77.2	77.3	0.3	147	9.5	97.5	0.525	1.87	150	55.51
0.29	49.4	74.0	73.7	73.7	73.8	0.3	151	9.2	93.0	0.487	1.88	131[e]	54.49
0.61	52.9	69.2	69.3	69.5	69.3	0.2	147	12	91.3	0.472	1.73	120	54.05
0.74	51.2	66.3	66.2	66.4	66.3	0.2	154	9.5	91.0	0.430	1.78	123	53.87
0.96	49.9	64.9	64.8	64.7	64.8	0.1	154	11	89.9	0.420	1.80	132	53.64

[a] M_{rs+} and M_{rs-} are the remanence values of the two intercepts with the vertical axis in the hysteresis loop.
[b] M_{rs} value in the B_{cr} measurement.
[c] Average of M_{rs+}, M_{rs-} and M_{rs_Bcr}.
[d] Difference between the largest and the smallest of the three M_{rs} estimates (M_{rs+}, M_{rs-} and M_{rs_Bcr})
[e] Average of slopes for 0, 0.61, 0.74 and 0.96 GPa.

subtracting the average slopes at the applied field of $|B| > 300$ mT (Fig. 3c). The hysteresis loop and hysteresis parameters of the plagioclase sample measured before and after the high-pressure experiments show almost the same features (Fig. 3d and Table 1), suggesting elastic behaviour of the sample within a pressure range of <1 GPa.

Figs 4(a) and (b) show hysteresis loops of the plagioclase sample at various pressures. The diamagnetic/paramagnetic corrections were successfully applied for the four cases of 0, 0.61, 0.74 and 0.96 GPa. However, it was difficult to estimate the slope for the case of 0.29 GPa because the magnetizations at $|B| > 300$ mT were too noisy. Consequently, the diamagnetic/paramagnetic slope value of 131 nAm^2 T^{-1} was adopted, which is the average value of the slopes of the other four measurements. The corrected hysteresis loops were almost the same for all pressure (Fig. 4a), but we observed a systematic decrease in M_{rs} with increasing pressure (Fig. 4b). This observation is consistent with the direct field demagnetization curves (Fig. 4c).

The hysteresis parameters determined from the obtained hysteresis loops are summarized in Table 2 and Fig. 5. B_c was determined by a second-degree polynomial interpolation within a range of $|B| < 110$ mT. The saturation remanence values of the upper (M_{rs+}) and lower (M_{rs-}) intercepts with the vertical axis in the hysteresis loop (Fig. 4b) and the M_{rs} value in B_{cr} measurement (M_{rs_Bcr}) are listed in Table 2. We calculated the average of the three values (M_{rs_ave}) as M_{rs} value. M_s was the average of the magnetizations for $|B| > 300$ mT. B_{cr} was determined by linear interpolation of two points immediately before and after the zero-crossing of the magnetization.

In order to evaluate the precision of the measurements, we calculated the standard deviation of M_s (σ_{Ms}) for $|B| > 300$ mT and the ΔM_{rs} value which was the difference between the largest and the smallest of the three M_{rs} estimates (M_{rs+}, M_{rs-} and M_{rs_Bcr}). The σ_{Ms} and ΔM_{rs} values were calculated to be ~10 and ~0.3 nAm^2, respectively (Table 2). Because the M_s and M_{rs} values should be constant in the measurements at constant pressure, it is reasonable to consider that the remanent and induced magnetizations can be measured with ~10 and ~0.3 nAm^2 precisions, respectively. The slope of the hysteresis loop at around B_c was calculated to be 1.3×10^{-6} Am^2 T^{-1} in the VSM measurement. The dispersion of ~10 nAm^2 in the magnetization measurements resulted in the dispersion of ~7.5 mT in the B_c values. The standard errors of B_c in the second-degree polynomial interpolation were less than 6.7 mT. On the basis of these precisions of the measurements, the pressure dependences of the hysteresis parameters are concluded as follows: B_c and M_s are at most ±5 per cent GPa^{-1} up to 1 GPa, whereas M_{rs} and B_{cr} decrease slightly with pressure at rates of −8 per cent GPa^{-1} and −18 per cent GPa^{-1}, respectively. In the pressure range <1 GPa, our results do not contradict those from the chiton teeth (Gilder *et al.* 2002, 2004), although mechanism dominating magnetic properties of the plagioclase sample was considered to be quite different from that of the chiton teeth sample.

5 DISCUSSION

Magnetic minerals contained in the plagioclase sample were well characterized by the microscopic and rock-magnetic observations. The minerals were nearly stoichiometric and non-interacting SD magnetite (ulvöspinel content $x = 0.05$–0.1, $M_{rs}/M_s = 0.45$ and $B_{cr}/B_c = 1.9$). Most of the SD magnetite grains had acicular shapes, while a small number of them displayed shapes that were nearly equidimensional. The low-temperature measurements with the MPMS showed consistent results with the above observations in terms of chemical composition, magnetic domain state and grain shape. Reliability of the hysteresis measurements using the MPMS combined with the high-pressure cell was confirmed by the VSM measurements. The hysteresis loop obtained using the high-pressure cell agrees with that obtained using the VSM. Therefore, it is reasonable to consider that reliable pressure dependences of the magnetic hysteresis parameters have been directly measured for SD magnetite.

Sato *et al.* (2014) conducted *in situ* magnetic hysteresis measurement under high pressures on MD magnetite using the same apparatus as used in this study. Change in the M_s value of MD magnetite is less than 1 per cent up to 1 GPa. The value of M_s of SD magnetite is not significantly affected by hydrostatic pressure up to 1 GPa, which is consistent with the MD results. As decreases in atomic distances are small within the pressure range <1 GPa (*cf.* bulk volume decreases by only –0.5 per cent GPa^{-1}, Haavik *et al.* 2000 and references therein), changes in superexchange interactions are considered too small to alter the saturation magnetization. This is consistent with the small pressure dependence of T_C (−2 per cent GPa^{-1}; Schult 1970), which is a direct measure of the strength of the exchange interaction (Dunlop & Özdemir 1997).

The value of B_c of SD magnetite is constant up to 1 GPa within experimental error, while that of MD magnetite monotonously increases with pressure at a rate of +91 per cent GPa^{-1} up to 1 GPa (Sato *et al.* 2014). The pressure effects on B_c for SD magnetite can be explained by considering the SD microcoercivity (B_K). A magnetization of an SD grain rotates from one stable direction to another when the applied field reaches a critical value B_K, and the bulk coercivity B_c is the average of B_K over randomly oriented grains (Dunlop & Özdemir 1997). In the case of acicular-shaped

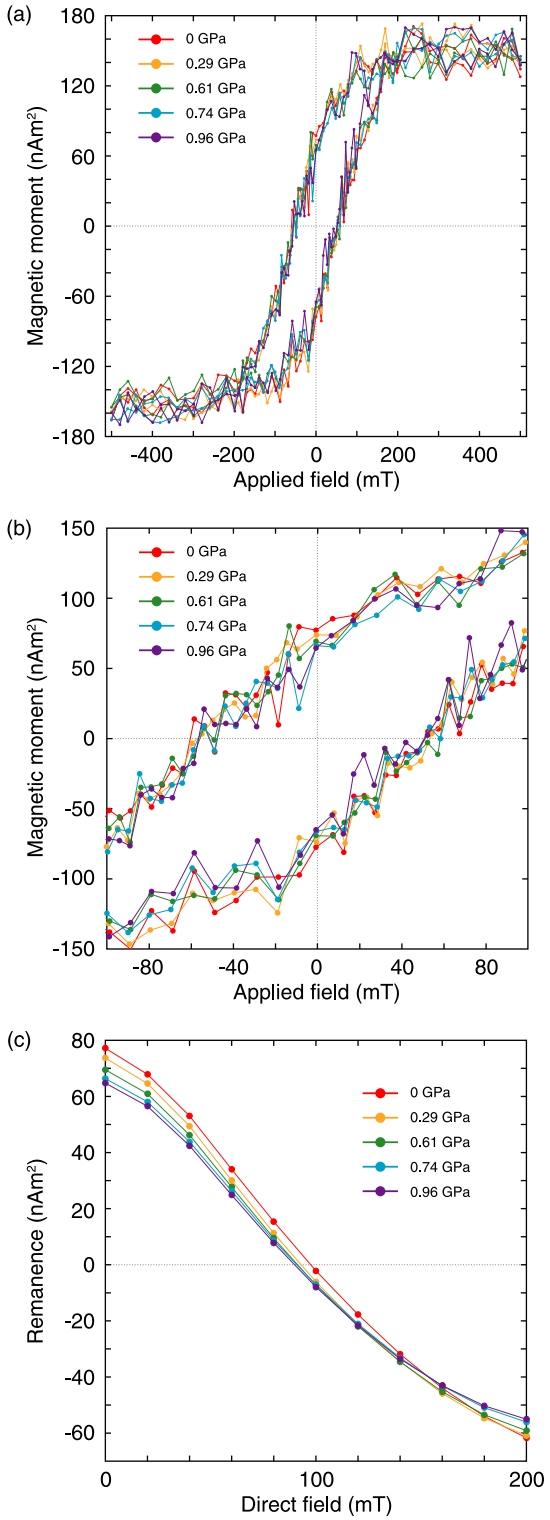

Figure 4. Magnetic hysteresis curves for the plagioclase sample. The hysteresis loops were corrected by subtracting diamagnetic/paramagnetic slopes. (a) Magnetic hysteresis loops, (b) enlarged view of the loops and (c) direct field demagnetization curves.

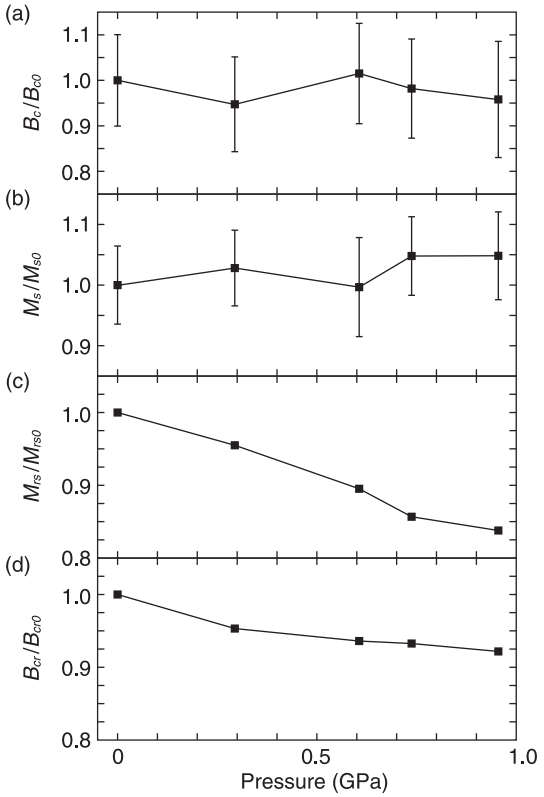

Figure 5. Pressure effect on the magnetic hysteresis parameters $B_c(P)/B_{c0}$, $M_s(P)/M_{s0}$, $M_{rs}(P)/M_{rs0}$ and $B_{cr}(P)/B_{cr0}$, where $X(P)$ represents a hysteresis parameter at pressure P and X_0 for an untreated sample (equivalent to $X(0)$). (a) $B_c(P)/B_{c0}$. The error bars express standard errors. (b) $M_s(P)/M_{s0}$. The error bars express standard deviations. (c) $M_{rs}(P)/M_{rs0}$. (d) $B_{cr}(P)/B_{cr0}$. M_{rs} and B_{cr}, estimated from magnetic remanence measurements, should be determined precisely because of the absence of induced magnetization by the high-pressure cell.

magnetite, B_K is proportional to $\Delta N \times M_s$, where ΔN is the difference between the self-demagnetization factors along the particle's long and short axes (Butler & Banerjee 1975). As the aspect ratio of a magnetite grain is unaffected by hydrostatic compression, it is expected that the value of B_c of acicular-shaped SD magnetite remains constant under hydrostatic pressurization.

Gradual decreases in M_{rs} and B_{cr} can be caused by the pressure effect on the first-order magnetic anisotropy constant K_1. Sawaoka & Kawai (1968) conducted systematic measurement of K_1 for some ferrites with spinel structure under hydrostatic pressure. They reported that the pressure dependences of K_1 for Fe_3O_4, $Fe_{2.96}Ti_{0.04}O_4$ and $Fe_{2.9}Ti_{0.1}O_4$ were -13.5×10^{-2} GPa^{-1}, -9.4×10^{-2} GPa^{-1} and -6.5×10^{-2} GPa^{-1}, respectively. In the case of nearly equidimensional SD magnetite, the following can be expected: (1) the threshold for superparamagnetic (SP) behaviour increases with pressure due to the decrease in an energy barrier imposed by the intervening [110] direction (eq. 17 in Butler & Banerjee 1975) and (2) the threshold for the SD–MD transition decreases with pressure due to the decrease in domain wall energy (eq. 9 in Butler & Banerjee 1975), resulting in the narrowing of the SD size range. Some of the equidimensional SD grains contained within the plagioclase sample might become SP or MD states under high pressure. Consequently, M_{rs} and B_{cr} are expected to decrease with pressure. In this model, B_c should also show a slight decrease with pressure because B_K is proportional to K/M_s in the case of nearly equidimensional SD magnetite (Dunlop & Özdemir 1997). Although B_c is constant within experimental error in this study, more precise determination of B_c would allow examination of whether the equidimensional grains affect the measurement results or not.

It is well known that deep crustal rocks contain various sizes of magnetite corresponding to domain states ranging from SD to MD (e.g. Dunlop & Özdemir 1997). For understanding the source of magnetic anomaly within the middle and lower crusts, it is important to know the magnetic properties of these magnetites under high pressure up to 1 GPa and high temperature near to T_C. Sato *et al.* (2014) estimated the relaxation time of remanent magnetization for MD magnetite based on the results of high-pressure experiments, which indicated that the relaxation times of MD magnetite below a few kilometres from the surface are shorter than 1 Myr. Thus, the pre-existing remanent magnetization of continental crusts below a few kilometres has been replaced by a viscous remanent magnetization acquired over the Brunhes chron, suggesting that MD magnetite contributes to the source of magnetic anomaly mainly in induced magnetization and viscous remanent magnetization.

In the present study, no significant pressure effects were detected for acicular SD magnetite within the pressure range <1 GPa. Therefore, temperature effects must govern the magnetic properties of middle and lower crustal rocks containing acicular SD magnetite. Acicular SD magnetite can preserve remanent magnetization over geological timescales under high temperature near to T_C (Pullaiah *et al.* 1975). Therefore, it is one of the important magnetic minerals carrying remanence-dominated magnetic anomaly. However, if the crustal rock contains a large amount of equidimensional SD magnetite grains, its magnetization might be reduced with depth because of the pressure effect as well as the temperature effect. This hypothesis should be tested in future studies using equidimensional SD magnetite samples. In the case that the magnetite grains contained in the middle and lower crustal rocks are identical to those of the plagioclase crystal used in this study, 4.4 and 6.6 per cent of M_{rs} decrease at depths of 20 and 30 km, respectively, which are the middle and lower crustal conditions. Because M_{rs} is a measure of the intensity of thermoremanent magnetization (e.g. eq. 8.21 in Dunlop & Özdemir 1997), remanent magnetization of the middle and lower crusts are, at least due to the pressure effect, several per cent lower than that of the upper crust. Such precise magnetic anomaly source modelling taking into account the effects of pressure and temperature should be possible in future study by using the pressure dependence data for SD magnetite (this study) and MD magnetite (Sato *et al.* 2014).

6 CONCLUSIONS

To investigate pressure effects on the magnetic properties of SD magnetite, *in situ* magnetic hysteresis measurements of SD magnetite under high pressures of up to 1 GPa were conducted, using the high-pressure cell specially designed for the MPMS. The natural plagioclase crystals containing nearly stoichiometric and non-interacting SD magnetite, which have been well characterized by the microscopic observation and the rock-magnetic measurements, were used as the experimental samples. It was found that B_c and M_s remained almost constant up to 1 GPa, while M_{rs} and B_{cr} decreased slightly with pressure at rates of −8 per cent GPa^{-1} and −18 per cent GPa^{-1}, respectively. These results can be interpreted by considering a mixture of acicular-shaped SD magnetite and small amount of nearly equidimensional SD magnetite: B_c, M_{rs} and B_{cr} for the former magnetite do not change with hydrostatic pressure, while those for the latter magnetite decrease with pressure because of the reduction in the magnetocrystalline anisotropy. Our results suggest that, in the middle and lower crusts, temperature effects mainly control the magnetic properties of acicular SD magnetite. In general, acicular SD magnetite can preserve remanent magnetization over geological timescales under high-temperature conditions; thus, it is one of the important magnetic minerals for a source of remanence-dominated magnetic anomaly.

ACKNOWLEDGEMENTS

We thank the two anonymous reviewers for their thoughtful and thorough reviews of the manuscript. We thank Dr. Hilal al Azri of the Ministry of Commerce and Industry of the Sultanate of Oman. This study was performed under the cooperative research program of Center for Advanced Marine Core Research (CMCR), Kochi University <Accept No. 10A017, 10B017, 11A016, 11B014, 12A027, and 12B024>. This research was supported by grant for the Global COE Program 'From the Earth to "Earths"' from the Ministry of Education, Culture, Sports, Science and Technology of Japan.

REFERENCES

Angel, R.J., 2004. Equations of state of plagioclase feldspars, *Contrib. Mineral. Petrol.,* **146,** 506–512.

Butler, R.F. & Banerjee, S.K., 1975. Theoretical single-domain grain size range in magnetite and titanomagnetite, *J. geophys. Res.,* **80**(29), 4049–4058.

Carmichael, R.S., 1969. Hydrostatic pressurization of magnetite, *Geophysics,* **34,** 775–779.

Carter-Stiglitz, B., Moskowitz, B., Solheid, P., Berquó, T.S., Jackson, M. & Kosterov, A., 2006. Low-temperature magnetic behavior of multidomain titanomagnetites: TM0, TM16, and TM35, *J. geophys. Res.,* **111,** B12S05, doi:10.1029/2006JB004561.

Christensen, N.I. & Mooney, W.D., 1995. Seismic velocity structure and composition of the continental crust: a global view, *J. geophys. Res.,* **100**(B6), 9761–9788.

Cisowski, S., 1981. Interacting vs. non-interacting single domain behavior in natural and synthetic samples, *Phys. Earth planet. Inter.,* **26,** 56–62.

Day, R., Fuller, M. & Schmidt, V., 1977. Hysteresis properties of titanomagnetites: grain-size and compositional dependence, *Phys. Earth planet. Inter.,* **13,** 260–267.

Dunlop, D.J. & Özdemir, Ö., 1997. *Rock Magnetism: Fundamentals and Frontiers,* Cambridge University Press, 573 pp.

Gee, J.S. & Kent, D.V., 2007. Source of oceanic magnetic anomalies and the geomagnetic polarity time scale, *Treatise on Geophysics,* **5,** 455–507.

Gilder, S.A., LeGoff, M., Chervin, J.-C. & Peyronneau, J., 2004. Magnetic properties of single and multi-domain magnetite under pressures from 0 to 6 GPa, *Geophys. Res. Lett.,* **31,** L10612, doi:10.1029/2004GL019844.

Gilder, S.A., LeGoff, M., Peyronneau, J. & Chervin, J., 2002. Novel high pressure magnetic measurements with application to magnetite, *Geophys. Res. Lett.,* **29,** 1392, doi:10.1029/2001GL014227.

Haavik, C., Stølen, S., Fjellvåg, H., Hanfland, M. & Häusermann, D., 2000. Equation of state of magnetite and its high-pressure modification: thermodynamics of the Fe-O system at high pressure, *Am. Mineral.,* **85,** 514–523.

Harrison, R.J. & Feinberg, J.M., 2008. FORCinel: an improved algorithm for calculating first-order reversal curve distributions using locally weighted regression smoothing, *Geochem. Geophys. Geosyst.,* **9,** Q05016, doi:10.1029/2008GC001987.

Heider, F., Dunlop, D.J. & Sugiura, N., 1987. Magnetic properties of hydrothermally recrystallized magnetite crystals, *Science,* **236,** 1287–1290.

Hodych, J.P., 1982. Magnetostrictive control of coercive force in multidomain magnetite, *Nature,* **298,** 542–544.

Hunt, C.P., Moskowitz, B.M. & Banerjee, S.K., 1995. Magnetic properties of rocks and minerals, in *Rock Physics and Phase Relations: A Handbook of Physical Constants,* Vol. 3, pp. 189–204, ed. Ahrens, T.J., American Geophysical Union.

Jennings, L.D. & Swenson, C.A., 1958. Effects of pressure on the superconducting transition temperatures of Sn, In, Ta, Tl, and Hg, *Phys. Rev.,* **112,** 31–43.

Kelemen, P.B., Koga, K. & Shimizu, N., 1997. Geochemistry of gabbro sills in the crust–mantle transition zone of the Oman ophiolite: implications for the origin of the oceanic lower crust, *Earth planet. Sci. Lett.,* **146,** 475–488.

Kirschvink, J. & Lowenstam, H., 1979. Mineralization and magnetization of chiton teeth: paleomagnetic, sedimentologic, and biologic implications of organic magnetite, *Earth planet. Sci. Lett.,* **44,** 193–204.

Kosterov, A., 2003. Low-temperature magnetization and AC susceptibility of magnetite: effect of thermomagnetic history, *Geophys. J. Int.,* **154,** 58–71.

McWhan, D.B. & Stevens, A.L., 1965. Effect of pressure on the magnetic properties and crystal structure of Gd, Tb, Dy, and Ho, *Phys. Rev.,* **139,** A682–A689.

Moskowitz, B.M., Frankel, R.B. & Bazylinski, D.A., 1993. Rock magnetic criteria for the detection of biogenic magnetite, *Earth planet. Sci. Lett.,* **120**(3), 283–300.

Moskowitz, B.M., Jackson, M. & Kissel, C., 1998. Low-temperature magnetic behavior of titanomagnetites, *Earth planet. Sci. Lett.,* **157,** 141–149.

Özdemir, Ö., Dunlop, D.J. & Moskowitz, B.M., 2002. Changes in remanence, coercivity and domain state at low temperature in magnetite, *Earth planet. Sci. Lett.,* **192,** 343–358.

Pullaiah, G., Irving, E., Buchan, K.L. & Dunlop, D.J., 1975. Magnetization changes caused by burial and uplift, *Earth planet. Sci. Lett.,* **28,** 133–143.

Roberts, A.P., Pike, C.R. & Verosob, K.L., 2000. FORC diagrams: a new tool for characterizing the magnetic properties of natural samples, *J. geophys. Res.,* **105,** 28 461–28 475.

Rudnick, R.L. & Fountain, D.M., 1995. Nature and composition of the continental crust: a lower crustal perspective, *Rev. Geophys.,* **33**(3), 267–309.

Rudnick, R.L. & Gao, S., 2003. Composition of the continental crust, *Treatise on Geochemistry,* **3,** 1–64.

Sato, M., Yamamoto, Y., Nishioka, T., Kodama, K., Mochizuki, N. & Tsunakawa, H., 2012. Pressure effect on low-temperature remanence of multidomain magnetite: change in demagnetization temperature, *Geophys. Res. Lett.,* **39,** L04305, doi:10.1029/2011GL050402.

Sato, M., Yamamoto, Y., Nishioka, T., Kodama, K., Mochizuki, N. & Tsunakawa, H., 2014. Hydrostatic pressure effect on magnetic hysteresis parameters of multidomain magnetite: implication for crustal magnetization, *Phys. Earth planet. Inter.,* **233,** 33–40.

Sawaoka, A. & Kawai, N., 1968. The effect of hydrostatic pressure on the magnetic anisotropy of ferrous and ferric ions in ferrites with spinel structure, *J. Phys. Soc. Japan,* **25,** 133–140.

Schult, A., 1970. Effect of pressure on the Curie temperature of titanomagnetites [$(1-x)\cdot Fe_3O_4-x\cdot TiFe_2O_4$], *Earth planet. Sci. Lett.,* **10,** 81–86.

Shive, P.N., Blakely, R.J., Frost, B.R. & Fountain, D.M., 1992. Magnetic properties of the lower continental crust, in *Continental Lower Crust,* pp. 145–177, eds Fountain, D.M., Arculus, R. & Kays, R.W., Elsevier.

SUPPORTING INFORMATION

Additional Supporting Information may be found in the online version of this paper:

Figure S1. Magnetic hysteresis curves for the high-pressure cell. (a) The hysteresis loop. (b) The hysteresis loop corrected by subtracting diamagnetic/paramagnetic slope. (http://gji.oxfordjournals.org/lookup/suppl/doi:10.1093/gji/ggv154/-/DC1).

Please note: Oxford University Press is not responsible for the content or functionality of any supporting materials supplied by the authors. Any queries (other than missing material) should be directed to the corresponding author for the paper.